

# Preparation of Superparamagnetic of $\text{Co}_{0.5}\text{Zn}_{0.5}\text{Fe}_2\text{O}_4$ at Room Temperature by Co-precipitation Method and Investigation of Its Physical Properties

S. Manouchehri<sup>\*1</sup>, M. H. Yousefi<sup>2</sup>, M. Mozaffari<sup>1</sup>, J. Amighian<sup>1</sup>

1- Department of Physics, Faculty of Science, University of Isfahan, Isfahan, I. R. Iran

2- Department of Physics, Malek-Ashtar University of Technology, Shahinshahr, Isfahan, I. R. Iran

(\*) Corresponding author: dez283@yahoo.com

(Received: 21 May 2009 and Accepted: 19 Apr. 2010)

## Abstract:

Magnetic nanoparticles of cobalt-zinc ferrite ( $\text{Co}_{0.5}\text{Zn}_{0.5}\text{Fe}_2\text{O}_4$ ) have been synthesized in a homogeneous aqueous solution at room temperature by co-precipitation method without any template and subsequent heat treatment. Synthesis of material is confirmed using XRD from the report of single phase polycrystalline ferrite material and also determined lattice constant. Atomic absorption spectrophotometer was used for the estimation of cobalt, zinc and  $\text{Fe}^{3+}$  ions. TEM micrograph shows that the nanoparticles are spherically shaped and the particle distribution is in the range between 6 to 10 nm. VSM shows that the sample is superparamagnetic at room temperature. The variation of AC-susceptibility of the samples with respect to temperature from 80 to 520 K was measured and it was found that the blocking temperature is around 195 K. TG-DTA studies confirmed the presence of associated water content in the precipitated nanoparticles and indicated that ferritization was completed. The FTIR spectra of  $\text{Co}_{0.5}\text{Zn}_{0.5}\text{Fe}_2\text{O}_4$  has been analyzed in the frequency range of 400-4000  $\text{cm}^{-1}$ .

**PACS:** 75.50.Gg; 75.50.Tt; 78.67.Bf

**Keywords:** Ferrite nanoparticles, Co-precipitation method, Superparamagnetism

## 1. INTRODUCTION

Magnetic nanoparticles are of great technological importance because of their use in magnetic fluid, information storage system, medical diagnostics, etc [1, 2]. Nanoparticle spinel oxides are attracting increasing interest in research because of their potential applications in nanoscience and technology and also for fundamental understanding of the strikingly different properties of the same material when the particle size approaches the atomic scale level [3, 4]. Some of the novel properties in magnetic nanoparticles, such as superparamagnetism (SPM), quantum magnetic tunneling, and surface spin

canting effect, have generated further interest in the study of nanoparticle spinels [3, 5].

Among spinel ferrites, cobalt ferrite,  $\text{CoFe}_2\text{O}_4$  is especially interesting because of their high cubic magnetocrystalline anisotropy, high coercivity, moderate saturation magnetization, high chemical stability, wear resistance and electrical insulation [6, 7]. Cobalt ferrites crystallize in an inverse spinel form [7].

According to their crystal structure, spinel-type ferrites have natural superlattice. They have tetrahedral A sites and octahedral B sites in  $\text{AB}_2\text{O}_4$  crystal structure. They show various magnetic

**Table 1:** Initial and estimated final cation concentrations of the prepared sample.

Cation concentration					
Co <sup>2+</sup>		Zn <sup>2+</sup>		Fe <sup>3+</sup>	
Initial	Final (estimated)	Initial	Final (estimated)	Initial	Final (estimated)
0.50	0.54	0.50	0.48	2.00	1.98

properties depending on the composition and cation distribution. Various cations can be placed in the A sites and B sites to tune its magnetic properties. Depending on the A site and B site cations, ferrimagnetic, antiferromagnetic, spin-(cluster) glass and paramagnetic behavior are observed in these spinel ferrites [8, 9]. These phenomena arise from finite size and surface effects that dominate the magnetic behavior of individual nanoparticles [10, 11]. Frenkel and Dorfman [11, 12] were the first who predict that a particle of ferromagnetic material, below a critical particle size (<15 nm for the common materials), would consist of a single magnetic domain, i.e. a particle that is a state of uniform magnetization at any field. The magnetization behavior of these particles above a certain temperature, i.e. the blocking temperature, is identical to that of the atomic paramagnets (superparamagnetism) except that an extremely large moment and thus, large susceptibilities are involved [11,13].

For SPM materials, the classical Langevin theory of paramagnetism applies with the only difference that the individual paramagnetic moments are not atomic moments (of the order of a few Bohr magnetons) but a particle can have a magnetic moment of several 100 or 1000 Bohr magnetons [4,14]. The field and the temperature dependence of the magnetization follow the expression:

$$M(H,T) = M_0 L(x)$$

Where  $L(x)=\coth x-1/x$  with  $x=\mu H/kT$  ( $\mu$  stands for the magnetic moment of an atom or a particle) is the Langevin function and  $M_0=n\mu$  ( $n$ =number of atoms/particles in a unit volume) is the saturation magnetization (magnetic moment per unit volume) of the ensemble of atoms/particles. It follows that there is no hysteresis (since the SPM state occurs when thermal energy overcomes the particles

anisotropy energy and the source of hysteresis is just the anisotropy) and there is no remanence. In addition, if SPM occurs then the magnetization is a function of  $H/T$  only. That is, the different  $M(H)$  curves measured at different temperatures as a function of  $H$  can be rescaled to a universal curve (the Langevin function) if  $M$  is plotted as a function of  $H/T$ . All this is valid only if there is no interaction among the SPM particles. If there is an interaction, hysteresis and remanence may occur. Allia et al. [15] who considered also the influence on the magnetic behavior of such interparticles interactions.

Many methods have been developed to prepare nanocrystalline [16]. Chemical precipitation and co-precipitation are the economical routes for the production of large quantities of nanosized ferrite particles [17, 18]. Other techniques such as sol-gel, mechanochemical processing, microemulsion and other physical methods have been also used to prepare these particles [19-21]. Chemical precipitation methods have been long used for the preparation of the magnetic nanoparticles, as the control over the particle size and shape can lead to the production of materials with desired magnetic properties [6, 17]. These methods offer many advantages over other methods, such as freedom from contamination, more homogenous mixing of the components and control over the particle size of the powders [17].

The purpose of this work is to prepare and characterize nanoparticles of cobalt-zinc ferrite ( $\text{Co}_{0.5}\text{Zn}_{0.5}\text{Fe}_2\text{O}_4$ ) at room temperature by co-precipitation method without subsequent calcination and as well as to investigate their magnetic properties. Characterization techniques like elemental analysis by atomic absorption spectrophotometer, thermal analysis using simultaneous TG-DTA, XRD, TEM, VSM and FTIR have been utilized.

## 2. EXPERIMENTAL

$\text{Co}_{0.5}\text{Zn}_{0.5}\text{Fe}_2\text{O}_4$  spinel ferrite nanocrystalline sample was prepared by co-precipitation method. A mixed solution of stoichiometric amounts of  $\text{CoCl}_2$ ,  $\text{ZnCl}_2$  and  $\text{FeCl}_3$  was prepared. This mixed solution was then added abruptly into NaOH solution, maintaining the pH at 12 under constant stirring at room temperature. The precipitation occurred immediately to change the reaction solution to dark brown colour solution. The precipitates were kept stirred in the reaction solution for 1 h at room temperature. The precipitate was filtered, washed with de-ionized water several times and then dried in air at room temperature.

X-ray diffraction analyses of the sample were carried out with a X-ray diffraction unit (Bruker, D8 ADVANCE) using Cu-K $\alpha$  ( $\lambda=1.54\text{\AA}$ ) radiation. The average crystallite size was calculated from X-ray line broadening using (311) peak and Scherrer's equation [22]. FTIR spectra of the sample were recorded in KBr medium in the range of 400–4000  $\text{cm}^{-1}$ . Thermal analysis (DTA and TG) of the sample were carried out with a thermal analyzer (Mettler Toledo Star System) in the temperature range of 300–1273 K, in air. Magnetization measurements were carried out at room temperature (300 K) with a Vibrating Sample Magnetometer (VSM) by varying the field from 0 to 1 T. The blocking temperature was determined from the temperature dependence of real part of the initial AC-susceptibility,  $\chi'$ . Measurements of  $\chi'$  were carried out at temperatures between 80 and 520 K in an AC-magnetic field of 200 A/m with a frequency of 100 kHz.

Transmission Electron Microscope (TEM) micrographs were recorded. Estimation of  $\text{Co}^{2+}$ ,  $\text{Fe}^{3+}$  and  $\text{Zn}^{2+}$  in the final product was carried out using atomic absorption spectrophotometer (Shimadzu, AA-680). Suitable lamps were used with wavelength 240.7, 248.3 and 213.9 nm for the estimation of cobalt, iron and zinc, respectively.

## 3. RESULTS AND DISCUSSIONS

Nanocrystalline  $\text{Co}_{0.5}\text{Zn}_{0.5}\text{Fe}_2\text{O}_4$  showed a cubic spinel structure from its XRD pattern (Figure 1). The crystallite size of the nanocrystalline precipitates was calculated by Scherrer formula [22]. It was found that the average crystallite size of this sample was less than 6 nm and TEM measurement (Figure 2) showed that the sample has an average particle size of <10 nm. Figure 3 shows the FTIR spectra of the ferrite sample. The presence of bands in the range of 400–600  $\text{cm}^{-1}$  (in the spectra), confirms the formation of the spinel phase. Some additional absorption bands around 3420  $\text{cm}^{-1}$  and 1630  $\text{cm}^{-1}$ , are present in the FTIR spectra of the sample. These bands correspond the stretching and bending modes of –OH group. From these results, it appears that hydroxyl groups are retained in the samples during preparation of the spinel ferrites by precipitation method. In order to investigate the nature of hydroxyl elimination during sintering of the dried precursor sample, DTA and TG were done on the sample. Figure 4 shows the DTA/TG curves of the dried precursor sample of  $\text{Co}_{0.5}\text{Zn}_{0.5}\text{Fe}_2\text{O}_4$ . DTA curve shows the presence of one endothermic and a broad hump exothermic peak at 150°C and 450°C, respectively, and TG curve shows that both of the peaks are accompanied with weight loss. The first endothermic peak appears to be due to loss of absorbed water. By annealing at temperature 450°C and 900°C, and XRD analysis, one can conclude that the second broad peak is related to the growth of particles and the formation of spinel phase is complete. The initial and final (estimated) cation concentrations of the prepared samples are given in Table 1. The initial ratio of  $(\text{Me}^{2+})/(\text{Fe}^{3+})$  was 0.5 and the ratio obtained from the final product was 0.515. The stoichiometry of cobalt-zinc ferrite did not deviate (within the allowed experimental errors including estimation of water content, dilution etc.) from their initial stoichiometry and matched well with the initial degree of substitution when was rounded to the first decimal.

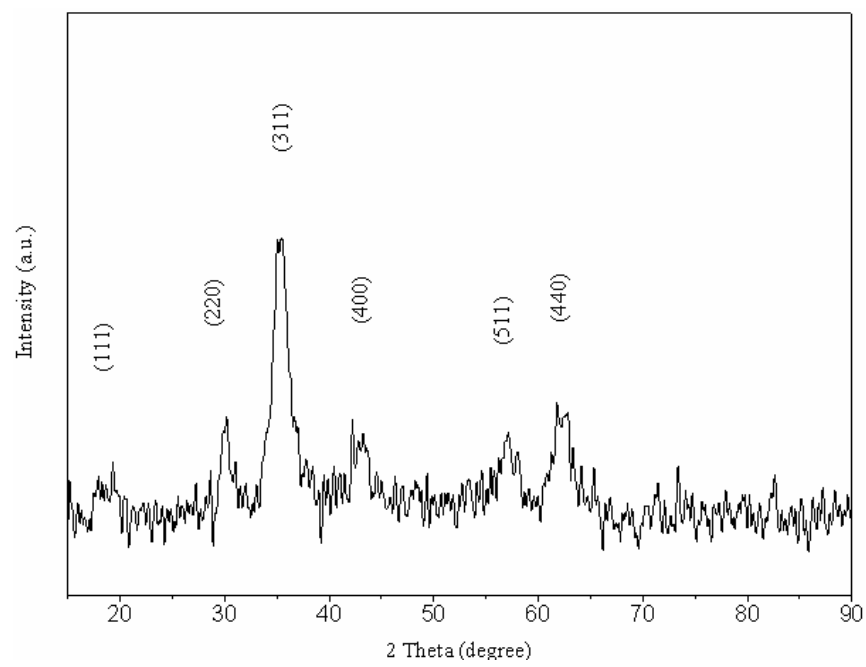


**Figure 1:** XRD pattern of the  $\text{Co}_{0.5}\text{Zn}_{0.5}\text{Fe}_2\text{O}_4$  sample at room temperature.

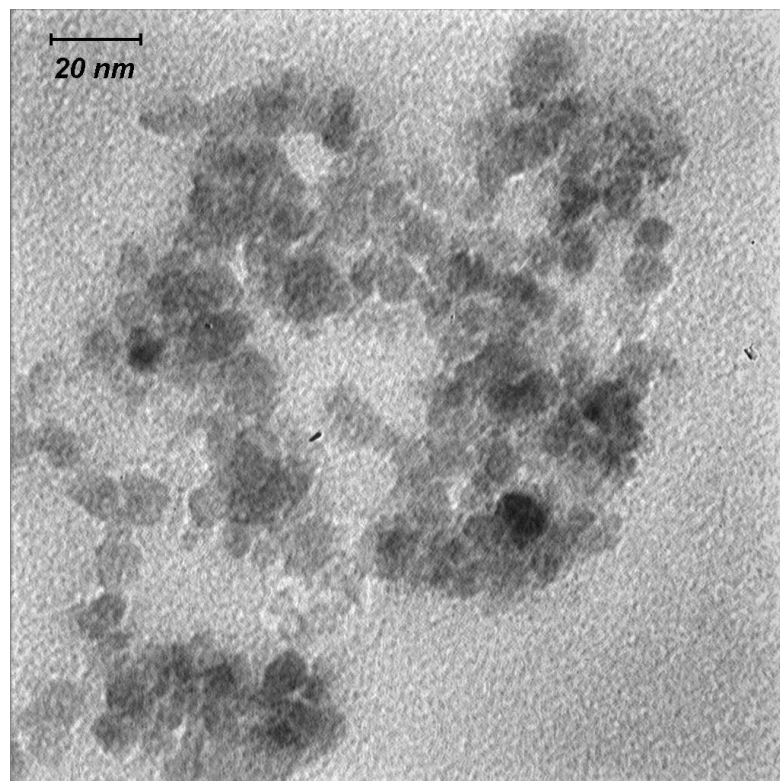


**Figure 2:** TEM micrograph of the  $\text{Co}_{0.5}\text{Zn}_{0.5}\text{Fe}_2\text{O}_4$  nanoparticles prepared at room temperature.

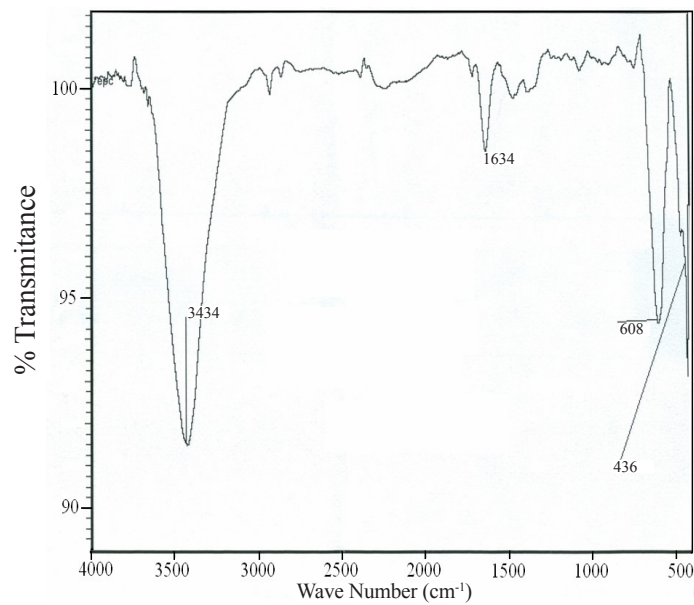


**Figure 3:** FTIR spectra of the  $\text{Co}_{0.5}\text{Zn}_{0.5}\text{Fe}_2\text{O}_4$  nanoparticles.

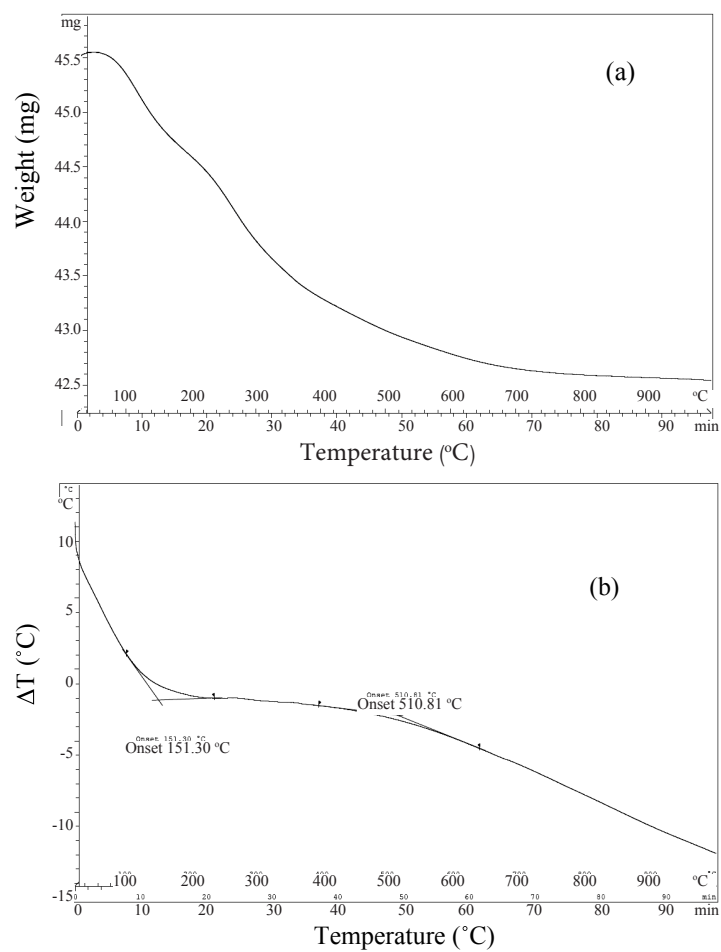


**Figure 4:** (a) Thermo gravimetric analysis and (b) DTA of  $\text{Co}_{0.5}\text{Zn}_{0.5}\text{Fe}_2\text{O}_4$  sample.

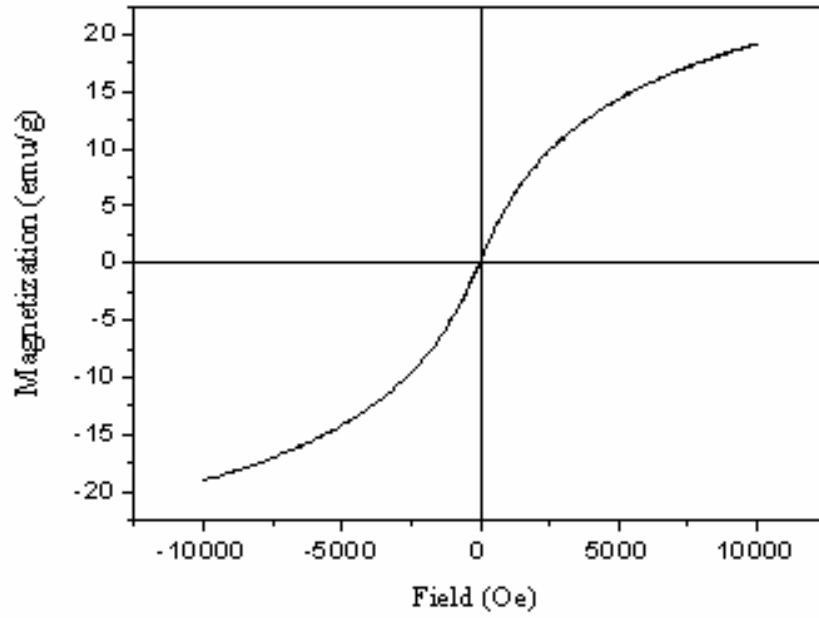


**Figure 5:** Magnetization curve of the  $Co_{0.5}Zn_{0.5}Fe_2O_4$  nanoparticles measured at room temperature.

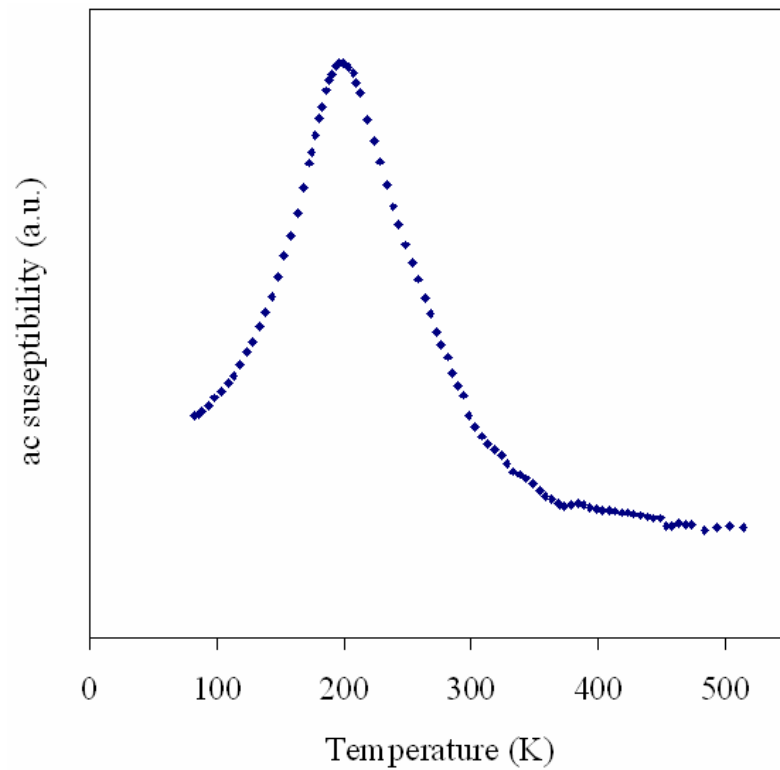


**Figure 6:** Temperature dependence of real part of AC-susceptibility data for the  $Co_{0.5}Zn_{0.5}Fe_2O_4$  nanoparticles at 100 kHz.

The room temperature magnetizations for applied magnetic field are shown in Figure 5. The magnetization for the sample is very weak and not saturated at the field of 10 kOe. This did not show any coercivity at this temperature. This is the characteristic of the superparamagnetism. This means that while the sample has the blocking temperature, at which the superparamagnetic relaxation starts to appear, below room temperature. Figure 6 shows the temperature dependence of the AC-susceptibility. We observe a maximum at a certain temperature TB (blocking temperature) that happen at 198 K. This result confirms the result of VSM and consequently we have superparamagnetism at room temperature. As expected, the AC-susceptibility reached to an approximately constant value as temperature increased due to paramagnetic behavior of the sample above its Curie temperature.

#### 4. CONCLUSIONS

- Preparation of  $\text{Co}_{0.5}\text{Zn}_{0.5}\text{Fe}_2\text{O}_4$  nanoparticles at room temperature is possible.
- $\text{Co}_{0.5}\text{Zn}_{0.5}\text{Fe}_2\text{O}_4$  may prepared in the average size rang less than 10 nm with uniform size distribution.
- The critical size for superparamagnetic of  $\text{Co}_{0.5}\text{Zn}_{0.5}\text{Fe}_2\text{O}_4$  at room temperature is less than 10 nm, while TB=198 K.
- Thermal analysis shows that the ferrite phase formed completely and didn't need any heat treatment for phase formation.
- Cobalt-zinc ferrite which prepared with this route has a good structural stability.

#### REFERENCES

1. R. Arulmurugan, G. Vaidyanathan, S. Sendhilnathan, B. Jeyadevan, *Physica B* 368 (2005) 223.
2. R. Arulmurugan, G. Vaidyanathan, S. Sendhilnathan, B. Jeyadevan, *J. Magn. Magn. Mater.* 303 (2006) 131.
3. R. N. Bhowmik, R. Ranganathan, S. Sarkar, C. Bansal, R. Nagarajan, *Phys. Rev. B* 68 (2003) 134433.
4. R. C. O'Handley, "Modern Magnetic Materials: Principles and Applications", Wiley, New York, 2000.
5. R. H. Kodama, A. E. Berkowitz, E. J. McNiff, Jr. Foner, S. Foner, *Phys. Rev. Lett.* 77 (1996) 394.
6. Y. I. Kim, D. Kim, Ch.S. Lee, *Physica B* 337 (2003) 42.
7. A. F. Júnior, E.C.O. Lima, M. A. Novak, P. R. Wells Jr, *J. Magn. Magn. Mater.* 308 (2007) 198.
8. A. K. M. Akther Hossain, H. Tabata, T. Kawai, *J. Magn. Magn. Mater.* 320 (2008) 1157.
9. L. K. Leung, B.J. Evans, A.h. Morish, *Phys. Rev. B* 8 (1) (1973) 29.
10. X. Batlle, A. Labarta, *J. Phys. D: Appl. Phys.* 35 (2002) R15.
11. P. Tartaj, M. P. Morales, S. Veintemillas-Verdaguer, T. González-Carreño, C. J Serna, *J. Phys. D: Appl. Phys.* 36 (2003) R182.
12. J. Frenkel, J. Dorfman, *Nature* 126 (1930) 274.
13. C. P. Bean, J. D. Livingston, *J. Appl. Phys.* 30 (1959) 1205.
14. B. D. Cullity, C. D. Graham, "Introduction to Magnetic Materials", 2nd edition, IEEE Press, John Wiley & Sons, New Jersey, 2009.
15. P. Allia, M. Coisson, P. Tiberto, F. Vinai, M. Knobel, M. A. Novak and W. C. Nunes, *Phys. Rev. B* 64 (2001) 144420.

16. G. V. Duong, R. Sato Turtelli, N. Hanha, D. V. Linh, M. Reissner, H. Michor, J. Fidler, G. Wiesinger, R. Grössinger, J. Magn. Magn. Mater. 307 (2006) 313.
17. J. Amighian, M. Mozaffari, B. Nasr, Phys. Stat. Sol. (c) 3 (2006) 3188.
18. D. H. Chen, X.R. He, Mater. Res. Bul. 36 (2001) 1369.
19. C. H. Peng, H. W. Wang, S.W. Kan, M. Z. Shen, Y. M. Wie, S.Y. Chen, J. Magn. Magn. Mater. 284 (2004) 113.
20. J. Ding, P.G. McCormick, R. Street, J. Magn. Magn. Mater. 171 (1997) 309.
21. J. Ding, X. Y. Liu, J. Wang, Y. Shi, Mater. Lett. 44 (2000) 19.
22. B. D. Cullity, "Elements of X-ray Diffraction", Addison-Wesley Publishing Company, Massachusetts, 1956.